

1 A Non-homogeneous Time Mixed Integer LP

2 Formulation for Traffic Signal Control

3 Iain Guilliard
4 National ICT Australia
5 7 London Circuit
6 Canberra, ACT, Australia
7 iguilliard@nicta.com.au

8 Scott Sanner
9 Oregon State University
10 1148 Kelley Engineering Center
11 Corvallis, OR 97331
12 scott.sanner@oregonstate.edu

13 Felipe W. Trevizan
14 National ICT Australia
15 7 London Circuit
16 Canberra, ACT, Australia
17 felipe.trevizan@nicta.com.au

18 Brian C. Williams
19 Massachusetts Institute of Technology
20 77 Massachusetts Avenue
21 Cambridge, MA 02139
22 williams@csail.mit.edu

23 5700 words + 7 figures + 0 table + 23 citations (Weighted total words: 7450 out of 7000 + 35
24 references)
25 July 31, 2015

1 ABSTRACT

2 We build on the body of work in mixed integer linear programming (MILP) approaches that at-
3 tempt to jointly optimize traffic signal control over an *entire traffic network* (rather than focus on
4 arterial routes) and specifically on improving the scalability of these methods for large urban traf-
5 fic networks. Our primary insight in this work stems from the fact that MILP-based approaches to
6 traffic control used in a receding horizon control manner (that replan at fixed time intervals) need to
7 compute high fidelity control policies only for the early stages of the signal plan; therefore, coarser
8 time steps can be employed to “see” over a long horizon to preemptively adapt to distant platoons
9 and other predicted long-term changes in traffic flows. To this end, we contribute the queue trans-
10 mission model (QTM) which blends elements of cell-based and link-based modeling approaches
11 to enable a non-homogeneous MILP formulation of traffic signal control. We then experiment with
12 this novel QTM-based MILP control in a range of networks demonstrating the improved scalabil-
13 ity possible with non-homogeneous time steps in comparison to the best homogeneous time step.
14 Our experiments also provide near-optimal traffic control policies for larger horizons and larger
15 networks than shown in previous implementations of MILP-based traffic signal control.

16 Using 204 words up to here. Maximum is 250 words.

17 1

¹Make sure to follow instructions and author guide: <http://onlinepubs.trb.org/onlinepubs/AM/InfoForAuthors.pdf> <http://onlinepubs.trb.org/onlinepubs/am/2015/WritingForTheTRRecord.pdf>

Also note this example related paper from Steve Smith (formatted to TRB specs): https://www.ri.cmu.edu/pub_files/2014/1/TRB14UTC.pdf

1 INTRODUCTION

2 As cities rapidly grow in population while urban traffic infrastructure often adapts at a slower pace,
 3 it is critical to maximize capacity and throughput of existing road infrastructure through optimized
 4 traffic signal control. Unfortunately, many large cities still use some degree of *fixed-time* control
 5 (e.g., Toronto (1)) even if they also use *actuated* or *adaptive* control methods such as SCATS (2)
 6 or SCOOT (3). However, there is further opportunity to improve traffic signal control even beyond
 7 adaptive methods through the use of *optimized* controllers as evidenced in a variety of approaches
 8 ranging from mixed integer (linear) programming (4, 5, 6, 7, 8, 9) to heuristic search (10, 11) to
 9 scheduling (12) to reinforcement learning (1). While such optimized controllers hold the promise
 10 of maximizing existing infrastructure capacity by finding more complex (and potentially closer to
 11 optimal) jointly coordinated intersection policies than arterially-focused master-slave approaches
 12 such as SCATS and SCOOT, such optimized methods are computationally demanding and either
 13 (a) do not guarantee jointly optimal solutions over a large intersection network (often because they
 14 only consider coordination of neighboring intersections or arterial routes) or (b) fail to scale to
 15 large intersection networks simply for computational reasons (which is the case for many mixed
 16 integer programming approaches).

17 In this work, we build on the body of work in mixed integer linear programming (MILP) ap-
 18 proaches that attempt to jointly optimize traffic signal control over an *entire traffic network* (rather
 19 than focus on arterial routes) and specifically on improving the scalability of these methods for
 20 large urban traffic networks. In our investigation of existing approaches in this vein, namely exem-
 21 plar methods in the spirit of (6, 8, 9) that use a (modified) cell transmission model (CTM) (13, 14)
 22 for their underlying prediction of traffic flows, we remark that a major drawback is the CTM-
 23 imposed requirement to choose a predetermined homogeneous (and often necessarily small) time
 24 step for reasonable modeling fidelity. This need to model large number of CTM cells with a small
 25 time step leads to MILPs that are exceedingly large and intractable to solve.

26 Our primary insight in this work stems from the fact that MILP-based approaches to traffic
 27 control used in a receding horizon control manner (that replan at fixed time intervals) need to
 28 compute high fidelity control policies only for the early stages of the signal plan; therefore, coarser
 29 time steps can be employed to “see” over a long horizon to preemptively adapt to distant platoons
 30 and other predicted long-term changes in traffic flows. This need for non-homogeneous control
 31 in turn spawns the need for an additional innovation: we require a traffic flow model that permits
 32 non-homogeneous time steps and properly models the travel time delay between lights. To this
 33 end, we might consider CTM extensions such as the variable cell length CTM (15), stochastic
 34 CTM extensions (16, 17), extensions for better modeling freeway-urban interactions (18) including
 35 CTM hybrids with link-based models (19), asymmetric CTMs for better handling flow imbalances
 36 in merging roads (20), the situational CTM for better modeling of boundary conditions (21), and
 37 the lagged CTM for improved modeling of the flow density relation (22). However, despite the
 38 widespread varieties of the CTM and the usage of the CTM (23) for a range of applications, there
 39 seems to be no extension that permits non-homogeneous time steps as required in our novel MILP-
 40 based control approach.

41 For this reason, as a major contribution of this work to enable our non-homogeneous
 42 time MILP-based model of joint intersection control, we contribute the queue transmission model
 43 (QTM) which blends elements of cell-based and link-based modeling approaches with the follow-
 44 ing key benefits:

- unlike previous joint intersection control work (6, 8, 9), it is inherently intended for *non-homogeneous* time steps that can be used for control over large horizons,
- any length of roadway with no merges or diverges can be modeled as a single queue leading to compact models of large traffic networks thus maintaining relatively compact MILPs for large traffic networks (i.e., large numbers of cells are not required between intersections), and
- it accurately models fixed travel time delays critical to green wave coordination as in (4, 5, 7) through the use of a non-first order Markovian update² model and combines this with the more global intersection signal optimization approach of (6, 8, 9).

In the remainder of this paper, we first formalize our novel QTM model of traffic flow with non-homogeneous time steps and show how to encode it as a linear program for simulating traffic. We proceed to allow the traffic signals to become discrete variables subject to a delay minimizing optimization objective and standard cycle and phase time constraints leading to our final MILP formulation of traffic signal control. We then experiment with this novel QTM-based MILP control in a range of networks demonstrating the improved scalability possible with non-homogeneous time steps in comparison to the best homogeneous time step. These experiments also provide near-optimal traffic control policies for larger horizons and larger networks than shown in previous implementations of MILP-based traffic signal control. ^{3 4 5}

THE QUEUE TRANSMISSION MODEL

A Queue Transmission Model (QTM) is the tuple $(\mathcal{Q}, \mathcal{L}, \vec{\Delta}t, \mathbf{I})$, where \mathcal{Q} and \mathcal{L} are, respectively, the set of queues and lights; $\vec{\Delta}t$ is a vector of size N representing the discretization of the simulation horizon $[0, T]$ and the duration in seconds of the n -th time interval is denoted as Δt_n ; and \mathbf{I} is a matrix $|\mathcal{Q}| \times T$ in which $I_{i,n}$ represents the flow of cars requesting to enter queue i from the outside of the network at time n .

A **traffic light** $\ell \in \mathcal{L}$ is defined as the tuple $(\Psi_\ell^{\min}, \Psi_\ell^{\max}, \mathcal{P}_\ell, \vec{\Phi}_\ell^{\min}, \vec{\Phi}_\ell^{\max})$, where:

- \mathcal{P}_ℓ is the set of phases of ℓ ;
- Ψ_ℓ^{\min} (Ψ_ℓ^{\max}) is the minimum (maximum) allowed cycle time for ℓ ; and
- $\vec{\Phi}_\ell^{\min}$ ($\vec{\Phi}_\ell^{\max}$) is a vector of size $|\mathcal{P}_\ell|$ and $\Phi_{\ell,k}^{\min}$ ($\Phi_{\ell,k}^{\max}$) is the minimum (maximum) allowed time for phase $k \in \mathcal{P}_\ell$.

²This is not explicitly mentioned later on

³Paper should follow the basic progression outlined in last paragraph above. Need to be careful to maintain the thread of the story throughout the paper and the summarize it in the conclusion with the major take-home results — longer horizons and larger networks for MILP-based control!

⁴We could really use some pictures in the Intro to refer to here and subsequently – both a traffic network divided into queues, and the concept of the piecewise linear evolution of traffic flow with **non-homogeneous** (dilated) time steps, something like I had provided in my early writeup. I think these help visually explain much of the context for the paper and its approach and are critical for reviewer understanding on a time budget for reading this They may only read the first 2-3 pages and then skim!

⁵A picture is worth a 1000 words but we only pay 250, hence a 4X ROI on pictures!

A **queue** $i \in \mathcal{Q}$ represents a segment of road that vehicles traverse at free flow speed; once traversed, the vehicles are vertically stacked in a stop line queue. Formally, a queue i is defined by the tuple $(Q_i, T_i^{\text{prop}}, F_i^{\text{out}}, \vec{F}_i, \vec{Pr}_i, \mathcal{Q}_i^{\mathcal{P}})$ where:

- Q_i is the maximum capacity of i ;
- T_i^{prop} is the time required to traverse i and reach the stop line;
- F_i^{out} represents the maximum traffic flow from i to the outside of the modeled network;
- \vec{F}_i and \vec{Pr}_i are vectors of size $|\mathcal{Q}|$ and their j -th entry (i.e., $F_{i,j}$ and $Pr_{i,j}$) represent the maximum flow from queue i to j and the turn probability from i to j ($\sum_{j \in \mathcal{Q}} Pr_{i,j} = 1$), respectively; and
- $\mathcal{Q}_i^{\mathcal{P}}$ denotes the set of traffic light phases controlling the outflow of queue i .

Differently than CTM (8, 13), QTM does not assume that $\Delta t_n = T_i^{\text{prop}}$ for all $n \in \{1, \dots, N\}$, that is, the QTM can represent non-homogeneous time intervals. The only requirement over Δt_n is that no traffic light maximum phase time is smaller than any Δt_n since phase changes occur only between time intervals; formally, $\Delta t_n \leq \min_{\ell \in \mathcal{L}, k \in \mathcal{P}_\ell} \Phi_{\ell,k}^{\max}$ for all $n \in \{1, \dots, N\}$.⁶

Traffic Flow Simulation with QTM

In this section, we present how to simulate traffic flow in a network using QTM and non-homogeneous time intervals Δt . We assume for the remainder of this section that a *valid* control plan for all traffic lights is fixed and given as parameter; formally, for all $\ell \in \mathcal{L}$, $k \in \mathcal{P}_\ell$, and interval $n \in \{1, \dots, N\}$, the binary variable $p_{\ell,k,n}$ is known a priori and indicates if phase k of light ℓ is active (i.e., $p_{\ell,k,n} = 1$) or not on interval n .

We represent the problem of finding the flow between queues as a Linear Program (LP) over the following variables defined for all interval $n \in \{1, \dots, N\}$ and queues i and j :

- $q_{i,n} \in [0, Q_i]$: traffic volume of queue i during interval n ;
- $f_{i,n}^{\text{in}} \in [0, I_{i,n}]$: inflow to the network via queue i during interval n ;
- $f_{i,n}^{\text{out}} \in [0, F_i^{\text{out}}]$: outflow from the network via queue i during interval n ; and
- $f_{i,j,n} \in [0, F_{i,j}]$: flow from queue i into queue j during interval n .

The maximum traffic flow from queue i to queue j is enforced by constraints (C1) and (C2). (C1) ensures that only the fraction $Pr_{i,j}$ of the total internal outflow of i goes to j , and (C2) forces the flow from i to j to be zero if all phases controlling i are inactive (i.e., $p_{\ell,k,n} = 0$ for all $k \in \mathcal{Q}_i^{\mathcal{P}}$). If more than one phase $p_{\ell,k,n}$ is active, then (C2) is subsumed by the domain upper bound of $f_{i,j,n}$.

$$f_{i,j,n} \leq Pr_{i,j} \sum_{k=1}^{|\mathcal{Q}|} f_{i,k,n} \quad (\text{C1})$$

$$f_{i,j,n} \leq F_{i,j} \sum_{p_{\ell,k,n} \in \mathcal{Q}_i^{\mathcal{P}}} p_{\ell,k,n} \quad (\text{C2})$$

⁶**To Iain:** Maybe bring forward a small network and any other figure that would help illustrate the model and comment about it.

1 To simplify the presentation of remainder of the LP, we define the helper variables $q_{i,n}^{\text{in}}$ (C3),
 2 $q_{i,n}^{\text{out}}$ (C4), $q_{i,n}^{\text{stop}}$ (C5) and t_n (C6) to represent the volume of traffic to enter, reach the stop line and
 3 leave queue i during interval n , and the time elapsed since the beginning of the simulation until the
 4 end of interval Δt_n . In order to account for the misalignment of the different Δt and T_i^{prop} , we need
 5 to find the volume of traffic that was able to arrive at queue i , traverse it (i.e., wait T_i^{prop} seconds),
 6 and reach the stop line before Δt_n is over. This volume of traffic is obtained by integrating over the
 7 current interval with the rate at which traffic was arriving during the intervals m to w containing
 8 the time $t_n - T_i^{\text{prop}}$ to $t_{n+1} - T_i^{\text{prop}}$. Where m is the interval such that $t_m \leq t_n - T_i^{\text{prop}} < t_{m+1}$,
 9 and w is the interval such that $t_w \leq t_{n+1} - T_i^{\text{prop}} < t_{w+1}$.⁷

$$10 \quad q_{i,n}^{\text{in}} = \Delta t_n (f_{i,n}^{\text{in}} + \sum_{j=1}^{|Q|} f_{j,i,n}) \quad (C3)$$

$$11 \quad q_{i,n}^{\text{out}} = \Delta t_n (f_{i,n}^{\text{out}} + \sum_{j=1}^{|Q|} f_{i,j,n}) \quad (C4)$$

$$12 \quad q_{i,n}^{\text{stop}} = \frac{t_{m+1} - t_n + T_i^{\text{prop}}}{\Delta t_m} q_{i,m}^{\text{in}} + \sum_{k=m+1}^{w-1} q_{i,k}^{\text{in}} + \frac{t_{n+1} - t_w - T_i^{\text{prop}}}{\Delta t_w} q_{i,w}^{\text{in}} \quad (C5)$$

$$13 \quad t_n = \sum_{x=1}^n \Delta t_x \quad (C6)$$

15 ⁸ The input rate of queue i during interval m is found by dividing $q_{i,m}^{\text{in}}$ with Δt_m , and then
 16 the total traffic arriving during the interval n is found by multiplying this rate by Δt_n . The flow
 17 conservation principle for non-homogeneous time steps is presented in (C7). If Δt is homogeneous
 18 for all n and T_i^{prop} is a multiple of Δt for all i , then (C5) reduces to $q_{i,n}^{\text{stop}} = q_{i,m}^{\text{in}}$ and (C7) reduces
 19 to $q_{i,n} = q_{i,n-1} - q_{i,n-1}^{\text{out}} + q_{i,m}^{\text{in}}$. To insure that the total volume of traffic travelling down the queue
 20 and waiting at the stop line does not exceed the capacity if the queue, we apply (C8).

$$21 \quad q_{i,n} = q_{i,n-1} - q_{i,n-1}^{\text{out}} + q_{i,n-1}^{\text{stop}} \quad (C7)$$

$$22 \quad \frac{t_n - t_{n+1} + T_i^{\text{prop}}}{\Delta t_w} q_{i,w}^{\text{in}} + \sum_{k=w+1}^n q_{i,k}^{\text{in}} + q_{i,n-1} \leq Q_i \quad (C8)$$

24 As with MILP formulations of CTM (e.g. Lin and Wang (8)), QTM is also susceptible to
 25 *withholding traffic*, i.e., the optimizer might prevent cars from moving from i to j even though
 26 the associated traffic phase is active and j is not full. We address this issue through our objective
 27 function (O1) by maximizing the total outflow $q_{i,n}^{\text{out}}$ (i.e., both internal and external outflow) of i
 28 plus the inflow $f_{i,n}^{\text{in}}$ from the outside of the network to i . This quantity is weighted by the remaining
 29 time until the end of the simulation horizon T to force the optimizer to allow as much traffic volume
 30 as possible into the network and move traffic to the outside the network as soon as possible. (O1)
 31 is analogous to minimizing delay in CTM models, e.g., (O1) is equivalent to the objective function

⁷To Iain: Triple check my explanation.

⁸To Felipe: Perhaps add this: Since the QTM is piecewise linear over an interval, the rate at which traffic enters a queue remains constant over the interval, and can be found by dividing $q_{i,m}^{\text{in}}$ by the Δt_m

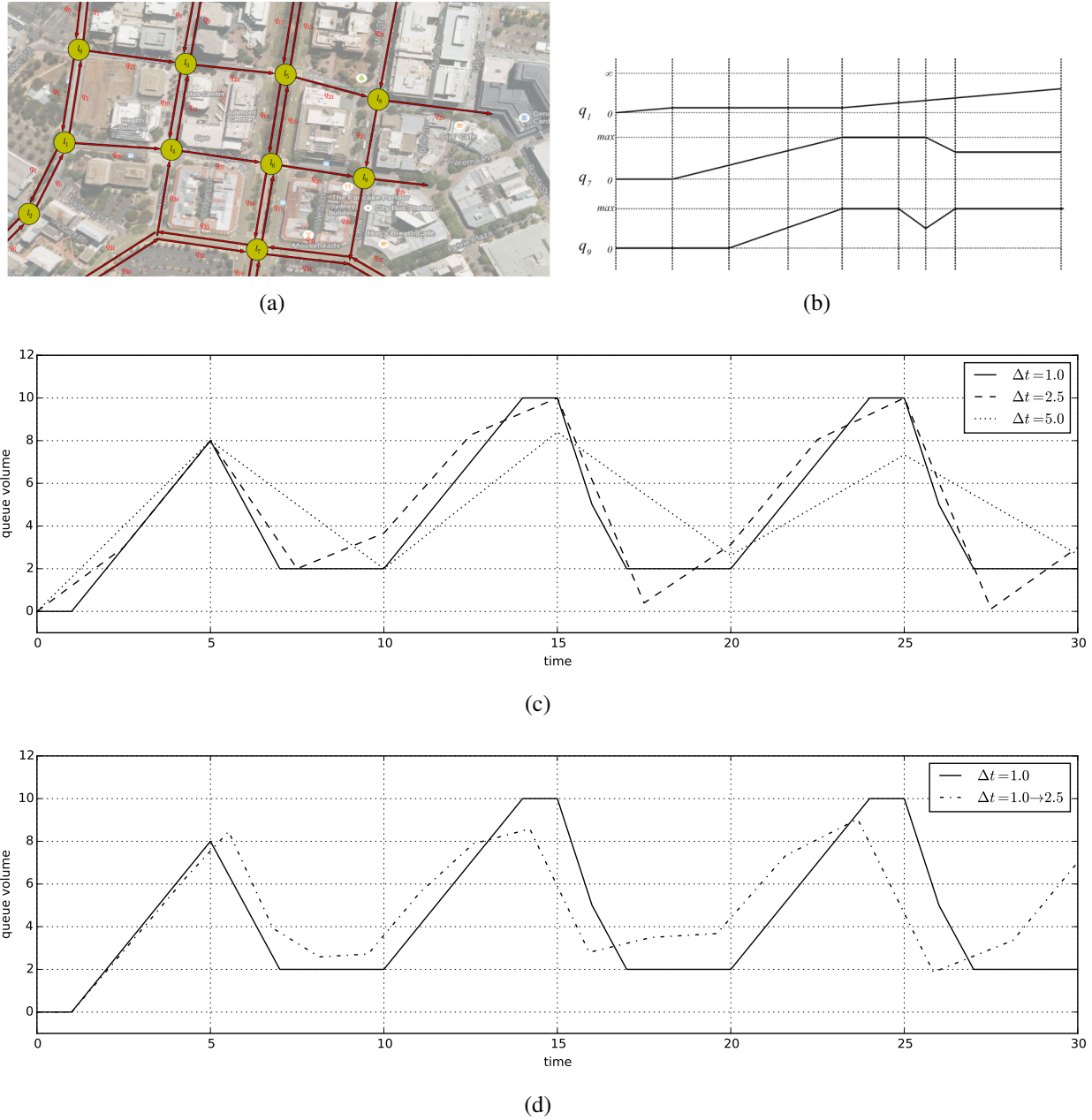


FIGURE 1 A QTM example showing the evolution of traffic volume in q_{27} over time. (a) Streetmap overlay showing how each queue in QTM network corresponds to a segment of roadway and each light to a controlled intersection. (b) Convergence with increasing refinement of Δt from 5.0 down to 1.0. (c) Dilation of Δt from 1.0 to 2.5 compared to a fixed Δt of 1.0.

- 1 (O3) in Lin and Wang (8) for their parameters $\alpha = \beta = 1$.⁹ Figure 5(d) shows the delay
- 2 experienced by each vehicle travelling along an avenue, where delay is the horizontal difference
- 3 between the cumulative departure and arrival curves at each point, less the free flow travel time

⁹To Iain: Add a paragraph linking the plots with the objective function.

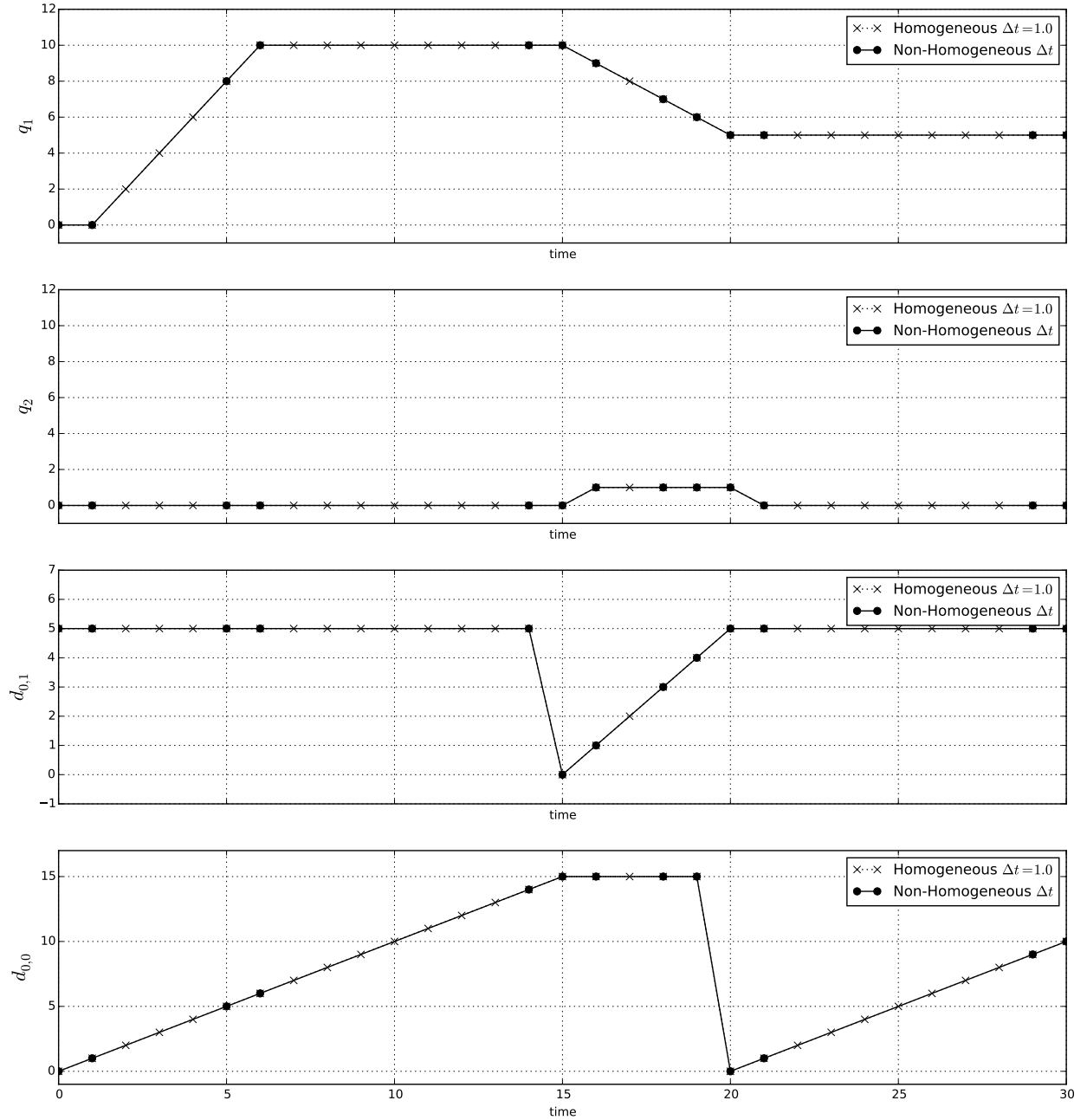


FIGURE 2 An example showing the convergence between a homogeneous solution with $\Delta t = 1.0$ and a non-homogeneous solution over 30 seconds for the same network. By using non-homogeneous time steps the same solution is found with only 14 sample points compared to 30 for homogeneous solution.

- 1 along the avenue. The objective function tries to maximise the arrival curve by pushing it up closer
- 2 to the departure curve, which also has the effect of minimising the horizontal distance, or delay.¹⁰

¹⁰Show diagrams with traffic predictions converging as time increment gets smaller. Validates that large time-steps are rough approximations while model behavior converges for small time steps.

$$\max \sum_{n=1}^N \sum_{i=1}^{|Q|} (T - t_n + 1)(q_{i,n}^{\text{out}} + f_{i,n}^{\text{in}}) \quad (\text{O1})$$

The objective function (O1) and constraints (C1–C8) form the LP representing the dynamic, piecewise linear model of flow in a QTM network over time when a control plan $p_{\ell,k,n}$ is given as an input parameter.

Figures 1(c), 1(d) and 2 show the results of applying the LP formulation to a simple model with a fixed signal plan, using both homogeneous Δt and non-homogeneous Δt .

TRAFFIC CONTROL WITH QTM AS AN MILP

In this section, we remove the assumption that a valid control plan for all traffic lights is given and extend the LP (O1, C1–C8) to an Mixed-Integer LP (MILP) that also computes the optimal control plan. Formally, for all $\ell \in \mathcal{L}$, $k \in \mathcal{P}_\ell$, and interval $n \in \{1, \dots, N\}$, the phase activation parameter $p_{\ell,k,n} \in \{0, 1\}$ becomes a free variable to be optimized. In order to obtain a valid control plan, we enforce that one phase of traffic light ℓ is always active at any interval n (C9) and that phase changes happen sequentially (C10), i.e., if phase k was active during interval $n - 1$ and has become inactive in interval n , then phase $k + 1$ must be active in interval n . (C10) assumes that $k + 1$ equals 1 if $k = |\mathcal{P}_\ell|$.¹¹

$$\sum_{k=1}^{|\mathcal{P}_\ell|} p_{\ell,k,n} = 1 \quad (\text{C9})$$

$$p_{\ell,k,n-1} \leq p_{\ell,k,n} + p_{\ell,k+1,n} \quad (\text{C10})$$

Next, we enforce the minimum and maximum phase durations (i.e., $\Phi_{\ell,k}^{\min}$ and $\Phi_{\ell,k}^{\max}$) for each phase $k \in \mathcal{P}_\ell$ of traffic light ℓ . To encode these constraints, we use the helper variable $d_{\ell,k,n} \in [0, \Phi_{\ell,k}^{\max}]$ defined by constraints (C11–C15) that: (i) holds the elapsed time since the start of phase k when $p_{\ell,k,n}$ is active (C11, C12) (Figure 3(a)); (ii) is constant and holds the duration of the last phase until the next activation when $p_{\ell,k,n}$ is inactive (C13, C14) (Figure 3(b)); and (iii) is restarted when phase k changes from inactive to active (C15) (Figure 3(c)). Notice that (C11–C15) employs the *big-M* method to turn the cases that should not be active into subsumed constraints based on the value of $p_{\ell,k,n}$. We use $\Phi_{\ell,k}^{\max}$ as our large constant since $d_{\ell,k,n} \leq \Phi_{\ell,k}^{\max}$ and $\Delta t_n \leq \Phi_{\ell,k}^{\max}$ by assumption (Section 2.1). Similarly, constraint (C16) ensures the minimum phase time of k and is not enforced while k is still active.

$$d_{\ell,k,n} \leq d_{\ell,k,n-1} + \Delta t_{n-1} p_{\ell,k,n-1} + \Phi_{\ell,k}^{\max} (1 - p_{\ell,k,n-1}) \quad (\text{C11})$$

$$d_{\ell,k,n} \geq d_{\ell,k,n-1} + \Delta t_{n-1} p_{\ell,k,n-1} - \Phi_{\ell,k}^{\max} (1 - p_{\ell,k,n-1}) \quad (\text{C12})$$

$$d_{\ell,k,n} \leq d_{\ell,k,n-1} + \Phi_{\ell,k}^{\max} p_{\ell,k,n-1} \quad (\text{C13})$$

$$d_{\ell,k,n} \geq d_{\ell,k,n-1} - \Phi_{\ell,k}^{\max} p_{\ell,k,n} \quad (\text{C14})$$

$$d_{\ell,k,n} \leq \Phi_{\ell,k}^{\max} (1 - p_{\ell,k,n} + p_{\ell,k,n-1}) \quad (\text{C15})$$

$$d_{\ell,k,n} \geq \Phi_{\ell,k}^{\min} (1 - p_{\ell,k,n}) \quad (\text{C16})$$

¹¹**To Iain:** I removed the constraint $p_{\ell,k,n} + p_{\ell,k+1,n} \leq 1$ because it is subsumed by $p_{\ell,k,n} \in \{0, 1\}$ and (C9)

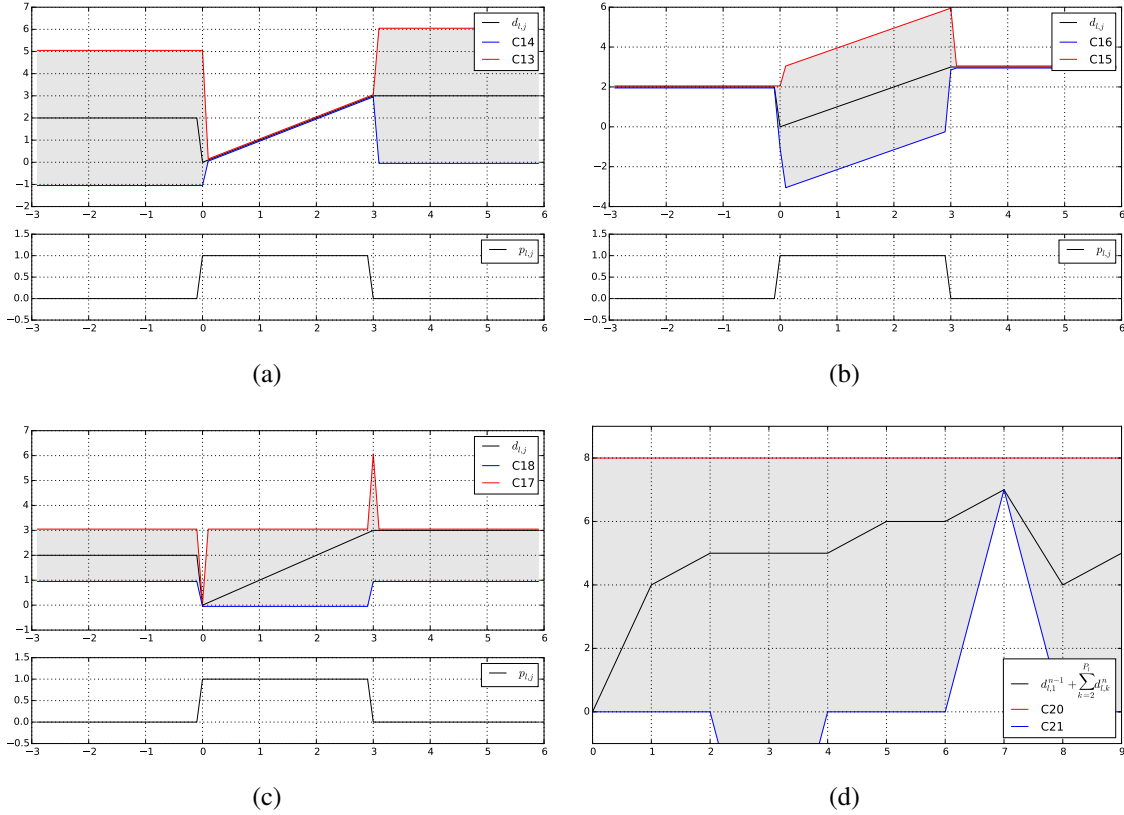


FIGURE 3 An example showing the phase and cycle time constraint envelopes. In (a), (b) and (c), $\Phi_{\ell,k}^{\min} = 1$ and $\Phi_{\ell,k}^{\max} = 3$, the duration of the previous activation was 2 and the duration of the current activation is 3. In (d), the total cycle time is 7 with $\Psi_{\ell}^{\min} = 7$, $\Psi_{\ell}^{\max} = 8$

Finally, we constrain the sum of all the phase durations for light ℓ to be within the cycle time limits Ψ_{ℓ}^{\min} (C17) and Ψ_{ℓ}^{\max} (C18) (Figure 3(d)). In both (C17) and (C18), we use the duration of phase 1 of ℓ from the previous interval $n - 1$ instead of the current interval n because (C15) forces $d_{\ell,1,n}$ to be 0 at the beginning of each cycle; however, from the previous end of phase 1 until $n - 1$, $d_{\ell,1,n-1}$ holds the correct elapse time of phase 1. Additionally, (C17) is enforced right after the end of the each cycle, i.e., when its first phase is changed from inactive to active.¹³

$$d_{\ell,1,n-1} + \sum_{k=2}^{|\mathcal{P}_{\ell}|} d_{\ell,k,n} \geq \Psi_{\ell}^{\min} (p_{k,1,n} - p_{k,1,n-1}) \quad (\text{C17})$$

$$d_{\ell,1,n-1} + \sum_{k=2}^{|\mathcal{P}_{\ell}|} d_{\ell,k,n} \leq \Psi_{\ell}^{\max} \quad (\text{C18})$$

The MILP that encodes the problem of finding the optimal traffic control plan in a QTM network is defined by (O1, C1–C18).

¹³**To Iain:** Relate the phase and cycle constraints with the plots

1 EMPIRICAL EVALUATION

2 In this section we compare the solutions for traffic networks modeled as a QTM using homoge-
 3 neous and non-homogeneous time intervals in two aspects: the quality of the solution and con-
 4 vergence to the **optimal solution**.¹⁴ We compare the quality of solutions based on the total travel
 5 time and we also consider the third quartile and maximum of the observed delay distribution. Our
 6 hypotheses are: (i) the quality of the non-homogeneous solutions is at least as good as the homoge-
 7 neous ones when the number of time intervals N is fixed; and (ii) the non-homogeneous approach
 8 requires less time intervals (i.e., smaller N) than the homogeneous approach to converge to the
 9 optimal solution. In the remainder of this section, we present the traffic networks considered in the
 10 experiments, our methodology, and the results.

11 Networks

12 We consider three networks of increasing complexity: an avenue crossed by three side streets; a 2-
 13 by-3 grid; and a 3-by-3 grid with a diagonal avenue. The queues receiving cars from outside of the
 14 network are marked in Figure 5 and we refer to them as input queues. The maximum capacity (Q_i)
 15 is 60 cars for non-input queues and **infinity** for input queues to prevent interruption of the input
 16 demand due to spill back from the stop line. The traversal time of each queue i (T_i^{prop}) is set at 9s (a
 17 distance of about 100m with a free flow speed of 50km/h). Flows are defined from the head of each
 18 queue i into the tail of the next queue j ; there is no turning traffic ($\text{Pr}_{i,j} = 1$), and the maximum
 19 flow rate between queues, $F_{i,j}$, is set at 5 cars/s. All traffic lights have two phases, north-south
 20 and east-west, and lights 2, 4 and 6 of network 3 have the additional northeast-southwest phase to
 21 control the diagonal avenue. For networks 1 and 2, $\Phi_{\ell,k}^{\min}$ is 1s, $\Phi_{\ell,k}^{\max}$ is 3s, Ψ_{ℓ}^{\min} is 2s, and Ψ_{ℓ}^{\max} is
 22 6s, for all traffic light ℓ and phase k . For network 3, $\Phi_{\ell,k}^{\min}$ is 1s and $\Phi_{\ell,k}^{\max}$ is 6s for all ℓ and k ; and
 23 Ψ_{ℓ}^{\min} is 2s and Ψ_{ℓ}^{\max} is 12s for all lights ℓ except for lights 2, 4 and 6 in which Ψ_{ℓ}^{\min} is 3s and Ψ_{ℓ}^{\max}
 24 is 18s.

25 Experimental Methodology

26 For each network, a constant background level traffic is injected in the network in the first 55s to
 27 allow the solver to settle on a stable policy. Then a spike in demand is introduced in the queues
 28 marked as ♠ from time 55s to 70s to trigger a policy change. From time 70s to 85s, the demand
 29 is returned to the background level, and then reduced to zero for all input queues. We extend the
 30 problem horizon T until all cars have left the network. By clearing the network, we can easily
 31 measure the total travel time for all the traffic as the area between the cumulative arrival and
 32 departure curves measured at the boundaries of the network.¹⁵ The background level for the input
 33 queues are 1, 4 and 2 cars/s for queues marked as ♦, ♣ and ♠, respectively; and during the high
 34 demand period, the queues ♠ receive 4 cars/s.

35 For both homogeneous and non-homogeneous intervals, we use the MILP QTM formula-
 36 tion (Section 3) in a receding horizon manner: a control plan is computed for a pre-defined horizon
 37 (smaller than T) and only a prefix of this plan is executed before generating a new control plan.
 38 Figure 4 depicts our receding horizon approach and we refer to the planning horizon as a major
 39 frame and its executable prefix as a minor frame. Notice that, while the plan for a minor frame is
 40 being executed, we can start computing the solution for the next major frame **based on a forecast**

¹⁴FWT: I don't think that optimal is the best word here since we arbitrarily fixed a value of Δt . Also, there is the technical problem that Gurobi might not have found the true optimal.

¹⁵FWT: is this explanation of how to compute the total travel time still necessary?

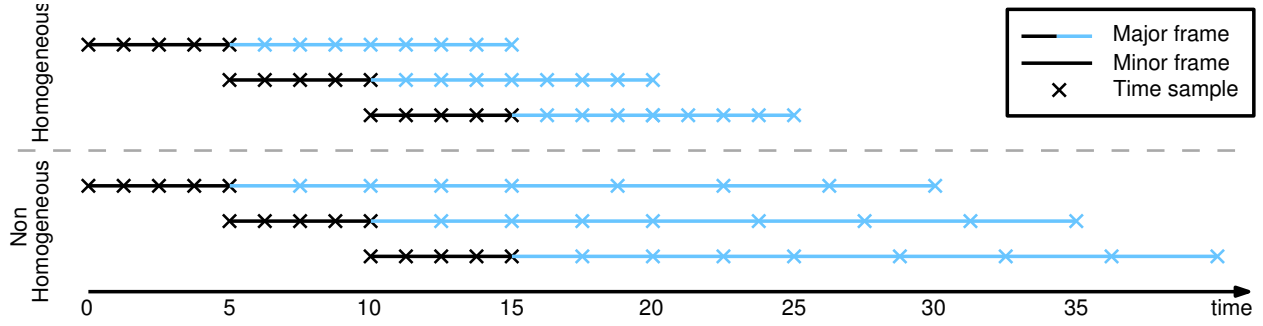


FIGURE 4 Receding horizon planning

1 **model**.¹⁶
 2 To perform a fair comparison between the homogeneous and non-homogeneous discretiza-
 3 tions, we fix the size of all minor frames to 10s and force it to be discretized in homogeneous
 4 intervals of 0.25s. For the homogeneous experiments, Δt is kept at 0.25s throughout the major
 5 frame; therefore, given N , the major frame size equals $N/4$ seconds for the homogeneous ap-
 6 proach. For the non-homogeneous experiments, Δt linearly increases from 0.25s at the end of
 7 the minor frame to 1.0s at the end of the major frame; therefore, the major frame size used by
 8 the non-homogeneous approach is $10.375 + 0.625(N - 40)$ seconds for a given $N > 40$. Once
 9 we have generated a series of minor frames, we concatenate them into a single plan and simulate
 10 the flow through the network using the QTM LP formulation with a fixed (homogeneous) Δt of
 11 0.25s.¹⁷ We also compare both receding horizon approaches against the **optimal** solution obtained
 12 by computing a single control plan for the entire control horizon (i.e., $[0, T]$) using a fixed Δt of
 13 0.25s.

14 For all our experiments, we used GurobiTM as MILP solver with 12 threads on a 3.1GHz
 15 AMD OpteronTM 4334 processor with 12 cores. We limit MIP gap accuracy to 0.1% and the time
 16 cutoff for solving a major frame to 3000s for the receding horizon approaches and unbounded for
 17 the optimal plan. All our results are averaged over five runs **to account for Gurobi's stochastic**
 18 **strategies**.

19 Results

20 Figures 6(a), 6(c) and 6(e) show, for each network, the increase in the total travel time w.r.t. the
 21 optimal solution as a function of N . As we hypothesized, the non-homogeneous discretization
 22 requires less time intervals to converge. This is important because the size of the MILP, including
 23 the number of binary variables, scales linearly with N ; therefore, the non-homogeneous approach
 24 can scale up better than the homogeneous one (e.g., Figure 6(e)).

25 The distribution of the total delay observed by each car while traversing the network is
 26 shown in Figures 6(b), 6(d) and 6(f). Each group of box plots represents a different value of N :
 27 when the non-homogeneous Δt first converges to the optimum solution; when the homogeneous
 28 Δt first converges on the optimum solution; and the optimum solution itself. In all networks, the
 29 quality of the solution obtained using non-homogeneous Δt is better or equal than using homo-
 30 geneous Δt for fixed N in both the total travel time and *fairness*, i.e., smaller third quartile and

¹⁶FWT: not sure if we should mention this.

¹⁷**Do we need to justify why we use the QTM as the simulator over say a micro simulator?**

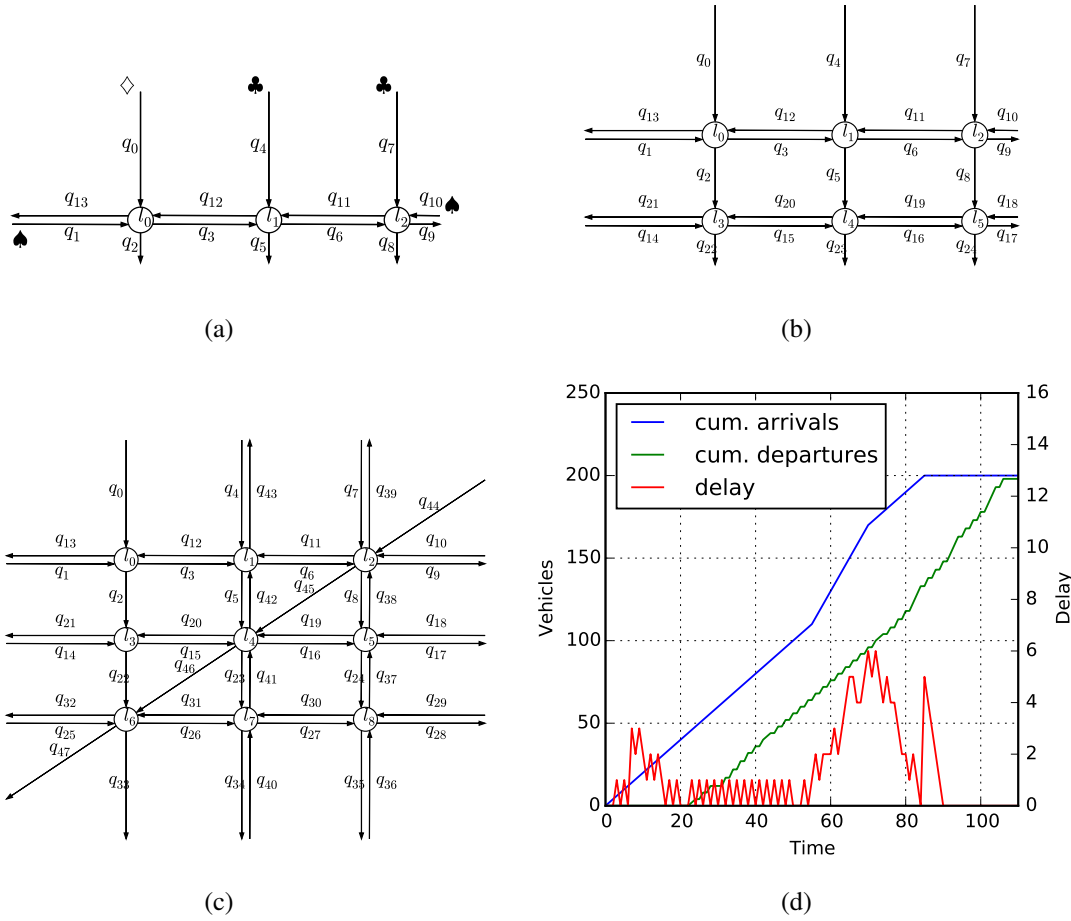


FIGURE 5 (a),(b),(c) Networks used in the evaluation of the QTM. (d) Cumulative arrival and departure curves for lane $q_1 \rightarrow q_3 \rightarrow q_6 \rightarrow q_9$ on network 2. Iain: please, mark the input queues.

- 1 maximum delay.
- 2 FWT: In the paragraphs above, we need to address network 2 because it is the exception
- 3 in both cases: in the end of Figure 6(c), homogeneous is better, and the homogeneous delay in
- 4 Figure 6(d) is also better.
- 5 Finally, Figure 7 shows the cumulative arrival and departure curves and the how delay
- 6 evolves over time for q_1 of network 2. Figure 7(a) shows the comparison at the point where the
- 7 non-homogeneous Δt first converges and shows that with the longer major frame time of the
- 8 non-homogeneous Δt , the solver is able to find a coordinated signal policy along the avenue to
- 9 dissipate the extra traffic that arrives at the 55s point, while the homogeneous Δt with its shorter
- 10 major frame fails to find a coordinated policy along the avenue and experiences more delay¹⁸.
- 11 Once the homogeneous Δt has converged in Figure 7(b), both solutions are close to the optimum
- 12 solution which is shown in Figure 7(c).¹⁹

¹⁸To Iain: I don't think that failure to coordinate is the best way to describe it because there is coordination but it happens too late.

¹⁹FWT: although Figure 7 is a nice illustration of how homogeneous and non-homogeneous differ, it is currently

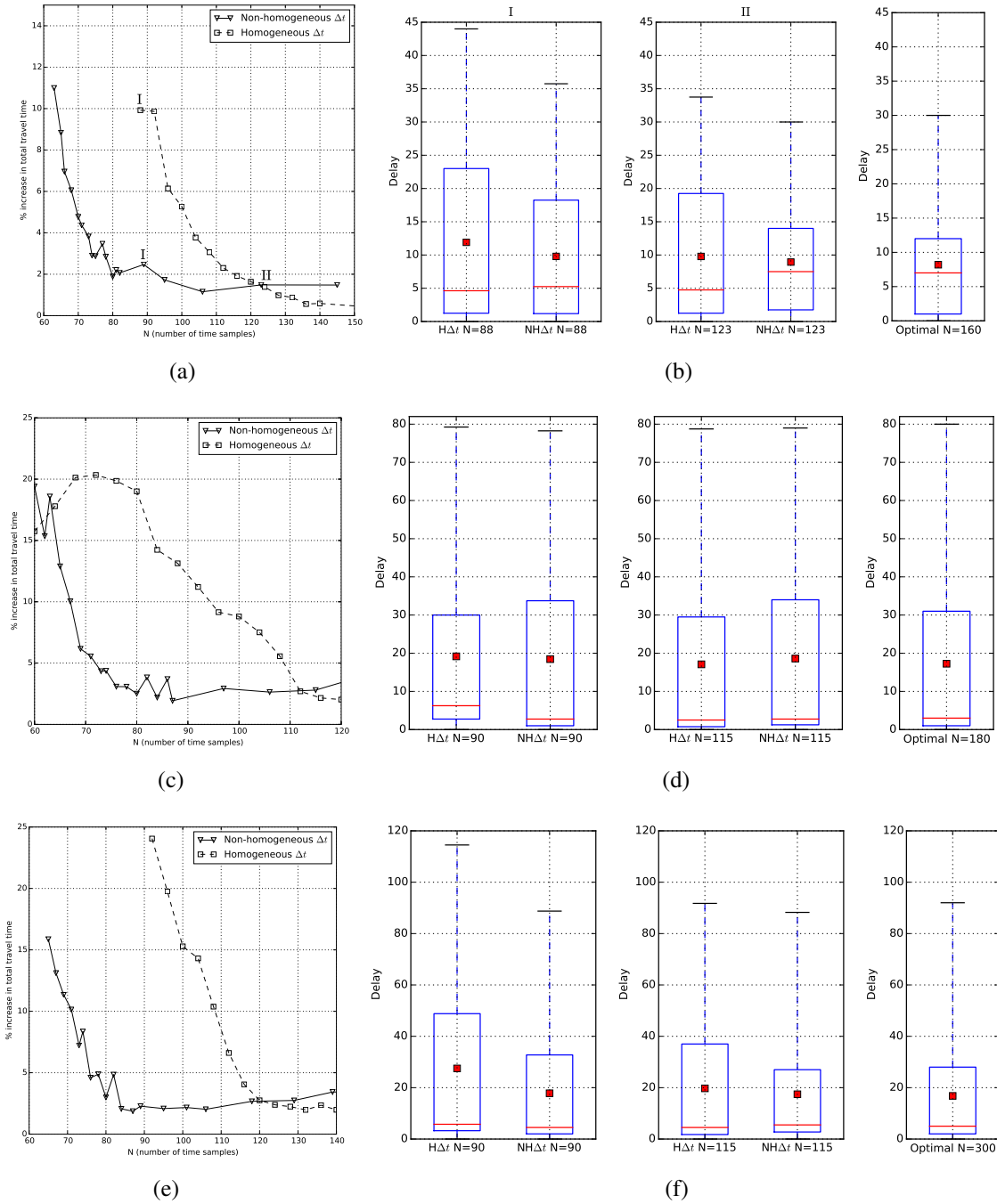


FIGURE 6 Results for the three networks showing the comparative % increase in total travel time for the network between using a homogeneous Δt and a non-homogeneous Δt , and the distribution of delay time at the convergence point of non-homogeneous Δt , the convergence point of homogeneous Δt and for the fully solved optimal solution. (a) and (b) 3 light avenue, (c) and (d) 6 light grid, and (e) and (f) 9 light grid.

not backing up any of our claims.

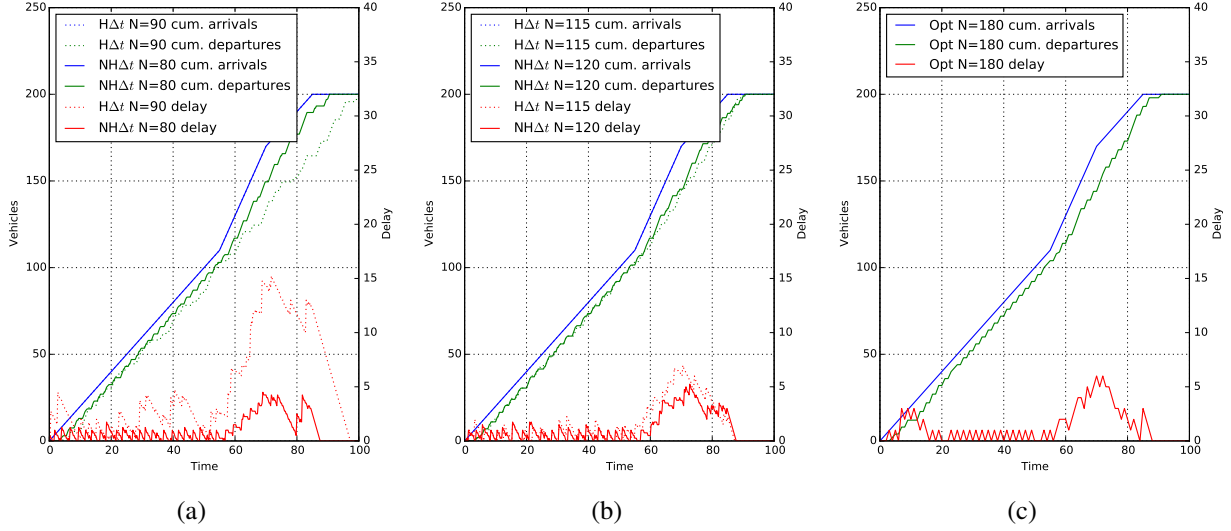


FIGURE 7 Cumulative arrival and departure curves and delay for queue 1 in the 6 light grid. (a) at the convergence point of the non-homogeneous Δt it is near to the optimum solution while homogeneous Δt lags behind (b) at the convergence point of homogeneous Δt both are near optimum, and (c) the fully solved optimal solution

CONCLUSION

In this paper, we showed how to formulate a novel queue transmission model (QTM) model of traffic flow with non-homogeneous time steps as a linear program. We then proceeded to allow the traffic signals to become discrete variables subject to a delay minimizing optimization objective and standard traffic signal constraints leading to a final MILP formulation of traffic signal control. We experimented with this novel QTM-based MILP control in a range of networks and demonstrated that by exploiting the non-homogeneous time steps supported by the QTM, we are able to scale the model up to larger networks whilst maintaining the same quality of a homogeneous solution using more binary variables.²⁰ Altogether, this work represents a major step forward in the scalability of MILP-based jointly optimized traffic signal control via the use of a non-homogeneous traffic models and thus helps pave the way for fully optimized joint urban traffic signal controllers as an improved successor technology to existing signal control methods.

REFERENCES

- [1] El-Tantawy, S., B. Abdulhai, and H. Abdelgawad, Multiagent reinforcement learning for integrated network of adaptive traffic signal controllers (MARLIN-ATSC): methodology and large-scale application on downtown toronto. *Intelligent Transportation Systems, IEEE Transactions on*, Vol. 14, No. 3, 2013, pp. 1140–1150.
- [2] Sims, A. G. and K. W. Dobinson, SCAT—The Sydney co-ordinated adaptive traffic system: Philosophy and benefits. *IEEE Transactions on Vehicular Technology*, Vol. 29, 1980.
- [3] Hunt, P. B., D. I. Robertson, R. D. Bretherton, and R. I. Winton, *SCOOT—A traffic responsive method of coordinating signals*. Transportation Road Research Lab, Crowthorne, U.K., 1981.

²⁰FWT: this is the first time we make the association between number time samples and binary variables

- [4] Gartner, N., J. D. Little, and H. Gabbay, *Optimization of traffic signal settings in networks by mixed-integer linear programming*. DTIC Document, 1974.
- [5] Gartner, N. H. and C. Stamatiadis, Arterial-based control of traffic flow in urban grid networks. *Mathematical and computer modelling*, Vol. 35, No. 5, 2002, pp. 657–671.
- [6] Lo, H. K., A novel traffic signal control formulation. *Transportation Research Part A: Policy and Practice*, Vol. 33, No. 6, 1998, pp. 433–448.
- [7] He, Q., K. L. Head, and J. Ding, PAMSCOD: Platoon-based Arterial Multi-modal Signal Control with Online Data. *Procedia-Social and Behavioral Sciences*, Vol. 17, 2011, pp. 462–489.
- [8] Lin, W.-H. and C. Wang, An enhanced 0-1 mixed-integer LP formulation for traffic signal control. *Intelligent Transportation Systems, IEEE Transactions on*, Vol. 5, No. 4, 2004, pp. 238–245.
- [9] Han, K., T. L. Friesz, and T. Yao, A link-based mixed integer LP approach for adaptive traffic signal control. *arXiv preprint arXiv:1211.4625*, 2012.
- [10] Lo, H. K., E. Chang, and Y. C. Chan, Dynamic network traffic control. *Transportation Research Part A: Policy and Practice*, Vol. 35, No. 8, 1999, pp. 721–744.
- [11] He, Q., W.-H. Lin, H. Liu, and K. L. Head, Heuristic algorithms to solve 0–1 mixed integer LP formulations for traffic signal control problems. In *Service Operations and Logistics and Informatics (SOLI), 2010 IEEE International Conference on*, IEEE, 2010, pp. 118–124.
- [12] Smith, S., G. Barlow, X.-F. Xie, and Z. Rubinstein, SURTRAC: Scalable Urban Traffic Control. In *Transportation Research Board 92nd Annual Meeting Compendium of Papers*, Transportation Research Board, 2013.
- [13] Daganzo, C. F., The cell transmission model: A dynamic representation of highway traffic consistent with the hydrodynamic theory. *Transportation Research Part B: Methodological*, Vol. 28, No. 4, 1994, pp. 269–287.
- [14] Daganzo, C. F., The cell transmission model, part II: network traffic. *Transportation Research Part B: Methodological*, Vol. 29, No. 2, 1995, pp. 79–93.
- [15] Xiaojian, H., W. Wei, and H. Sheng, Urban traffic flow prediction with variable cell transmission model. *Journal of Transportation Systems Engineering and Information Technology*, Vol. 10, No. 4, 2010, pp. 73–78.
- [16] Sumalee, A., R. Zhong, T. Pan, and W. Szeto, Stochastic cell transmission model (SCTM): A stochastic dynamic traffic model for traffic state surveillance and assignment. *Transportation Research Part B: Methodological*, Vol. 45, No. 3, 2011, pp. 507–533.
- [17] Jabari, S. E. and H. X. Liu, A stochastic model of traffic flow: Theoretical foundations. *Transportation Research Part B: Methodological*, Vol. 46, No. 1, 2012, pp. 156–174.

- 1 [18] Huang, K. C., *Traffic Simulation Model for Urban Networks: CTM-URBAN*. Ph.D. thesis,
2 Concordia University, 2011.
- 3 [19] Muralidharan, A., G. Dervisoglu, and R. Horowitz, Freeway traffic flow simulation using the
4 link node cell transmission model. In *American Control Conference, 2009. ACC'09.*, IEEE,
5 2009, pp. 2916–2921.
- 6 [20] Gomes, G. and R. Horowitz, Optimal freeway ramp metering using the asymmetric cell trans-
7 mission model. *Transportation Research Part C: Emerging Technologies*, Vol. 14, No. 4,
8 2006, pp. 244–262.
- 9 [21] Kim, Y., *Online traffic flow model applying dynamic flow-density relation*. Int. At. Energy
10 Agency, 2002.
- 11 [22] Lu, S., S. Dai, and X. Liu, A discrete traffic kinetic model—integrating the lagged cell trans-
12 mission and continuous traffic kinetic models. *Transportation Research Part C: Emerging*
13 *Technologies*, Vol. 19, No. 2, 2011, pp. 196–205.
- 14 [23] Alecsandru, C., A. Quddus, K. C. Huang, B. Rouhieh, A. R. Khan, and Q. Zeng, An as-
15 sessment of the cell-transmission traffic flow paradigm: Development and applications. In
16 *Transportation Research Board 90th Annual Meeting*, 2011, 11-1152.